UDK 620.1:669.721.5:544.653.23
Original scientific article/Izvirni znanstveni članek

ISSN 1580-2949
MTAEC9, 53(2).225(2019)

FORMATION OF A COMPOSITE ANODIC OXIDATION FILM CONTAINING Al_2O_3 PARTICLES ON THE AZ31 MAGNESIUM ALLOY

TVORBA KOMPOZITNEGA ANODNEGA OKSIDNEGA FILMA Z Al_2O_3 DELCI NA MAGNEZIJEVI ZLITINI AZ31

Gou Yinning[1,2*], Su Yongyao[3], Chai Linjiang[1*], Zhi Yan[1], Lai Siying[1], Xiong Min[1]

[1]Chongqing University of Technology, School of Material Science and Engineering, no. 69 Hongguang Avenue, Banan District, Chongqing 400054, China
[2]Chongqing University of Technology, Chongqing Key Laboratory of Mold Technology, no. 69 Hongguang Avenue, Banan District, Chongqing 400054, China
[3]Chongqing University of Arts and Sciences, Research Institute for New Material Technology, no. 319 Honghe Avenue, Yongchuan District, Chongqing 402160, China

Prejem rokopisa – received: 2018-07-05; sprejem za objavo – accepted for publication: 2018-11-06

doi:10.17222/mit.2018.136

A composite film containing Al_2O_3 nanoparticles was successfully anodized on the AZ31 alloy using an alkaline NaOH–Na_2SiO_3 solution. The formation process and the mechanism of the nanoparticles were investigated by means of XRD, SEM and EDS characterization. The addition of nanoparticles does not change the basic process of anodizing magnesium alloys. The thickness change of the oxide films is consistent with the voltage variation and the oxidation time. During the first 5 seconds of anodization, the sample weight decreases, indicating that Mg dissolution dominates this process. Subsequently, the sample weight begins to increase and the film development plays an important role. The oxide film is formed by Al_2O_3 nanoparticles absorbed on the surface of the magnesium matrix. The nanoparticles have been involved in the growth process of the oxide films. The composite oxide film is composed of MgO, Mg_2SiO_4 and α-Al_2O_3 phases. In the process of composite oxidation, Al_2O_3 nanoparticles can fill in the pores and the cracks of the oxide films after being absorbed on the surface of the film. In addition, they can also be continuously captured in the oxide film, forming an oxide film structure reinforced by Al_2O_3 nanoparticles and leading to enhanced performance.

Keywords: magnesium alloy, composite oxide film, Al_2O_3 particles, formation

Avtorji opisujejo uspešni nastanek kompozitnega filma, ki vsebuje Al_2O_3 nanodelce na površini Mg zlitine AZ31 s pomočjo anodne oksidacije v alkalni raztopini NaOH-Na_2SiO_3. Potek in mehanizem nastanka nanodelcev so raziskovali in okarakterizirali z uporabo XRD, SEM in EDS. Dodatek nanodelcev ni spremenil osnovnega procesa anodizacije Mg zlitin. Debelina oksidnega filma se ujema s spremembo električne napetosti in časa oksidacije. Prvih 5 sekund anodizacije se masa vzorcev manjša, kar kaže na to, da dominira proces raztapljanja Mg. Sledi naraščanje mase vzorcev, kar pomeni, da pomembno vlogo v procesu predstavlja tvorba oksidnega filma. Nastali oksidni film vsebuje nanodelce Al_2O_3, absorbirane na površini v Mg matrici. Nanodelci so vključeni v proces rasti oksidnega filma. Kompozitni oksidni film je sestavljen iz MgO, Mg_2SiO_4 in α-Al_2O_3. V procesu nastajanja oksidnega filma nanodelci Al_2O_3 zapolnijo pore in razpoke potem, ko se absorbirajo na površino filma. Dodatno so lahko le-ti stalno ujeti v oksidnem filmu, kar ojača njegovo strukturo in izboljša njegove lastnosti.

Ključne besede: zlitina na osnovi magnezija, kompozitni oksidni film, nastanek Al_2O_3 delcev

1 INTRODUCTION

Due to the urgent need for environmental protection and energy saving, lightweight automobiles have become the main trend in the world of automobile development. Magnesium alloys are ideal materials for the automotive industry due to their unique properties, including an extremely low density, a high strength-to-weight ratio, an excellent thermal conductivity and an easy recyclability.[1,2] However, their applications are restricted by poor corrosion and wear resistance. Some surface-modification processes like laser cladding,[3] sol-gel coatings,[4] chemical conversion coatings,[5] plasma-enhanced chemical vapor deposition,[6] anodizing,[7] micro-arc oxidation[8] and composite treatments,[9] have been attempted to improve the surface properties. Among them, the anodic oxidation treatment has been proved to be one of the most promising methods. In order to improve the properties of oxide films, different nanoparticle additives suspended in the electrolyte were incorporated into the film to produce optimized microstructures. Such particles include SiC,[10] TiO_2,[11] ZrO_2,[12] CeO_2,[13] Al_2O_3,[14] and graphene.[15] Lu et al. found that the photocatalytic activity was achieved via the introduction of anatase (TiO_2 particles) to the plasma electrolytic oxidation bath.[11] Wang reported that nano Al_2O_3 powers greatly improved the hardness and the anti-corrosion properties of a micro-arc oxidation film on the AZ91D Mg alloy.[14] Research from Chen et al. showed that the corrosion resistance of the composite oxidation coatings with graphene particles increased greatly.[15] Obviously, adding nanoparticle additives to the electrolyte is an effective way to improve the perform-

*Corresponding authors e-mail:
chailinjiang@cqut.edu.cn (Chai Linjiang)

ance of the anodic oxidation film. In spite of many efforts in this respect, the particle additives' incorporation mechanism during oxidation has rarely been explored. The mechanical trapping of particles was noted in the traditional coating-preparation techniques from a liquid solution (like electroplating and anodizing) to form a composite coating.[16] However, the anodic oxidation on the magnesium alloy is a process distinct from those conventional electrochemical coating processes.

In this study, Al_2O_3 particles were added to a NaOH–Na_2SiO_3 electrolyte to prepare anodic oxidation films on the AZ31 magnesium alloy. To further understand the film formation after adding the Al_2O_3 particles to the electrolyte, variations of the voltage and the oxide film characteristics (thickness and morphology) with time were studied.

2 MATERIALS AND METHODS

The commercially available AZ31 alloy with dimensions of (20 × 20 × 2) mm was used for this study. The samples were ground to 2000 grit using silicon carbide papers, ultrasonically cleaned with acetone and distilled water, and then dried in the air.

Based on our previous studies,[17–20] an environmentally friendly NaOH–Na_2SiO_3 alkaline electrolyte containing 5 g/L of sodium hydroxide, 5 g/L of ethylene diamine and tetra acetic acid, 15 g/L of phytic acid, and 120 g/L of sodium silicate was selected for the anodizing treatment in the present work. A total of 10 g/L of Al_2O_3 particles with a mean particle size of 300 nm (**Figure 1**) were introduced into the electrolyte to produce the composite coatings. The AZ31 specimens were used as the anode with two AISI 316L panels as the cathode. The anodizing process was conducted at a constant current density (10 mA/cm^2). The temperature of the electrolytic solution was kept at 20 °C for 20 min.

To make the Al_2O_3 nanoparticles fully dispersed in the aqueous solution, a small amount of distilled water and anionic surfactant (0.06 g/L) were added to the Al_2O_3 particles. The mixture was then subjected to ultrasonic dispersion for 30 min. Subsequently, the mixture was poured into the anodic oxidation electrolyte. Then, it was stirred for 20 min with a magnetic stirrer to make the Al_2O_3 particles fully suspended and dispersed in the solution. During the anodizing process, the bath solution was also stirred with a magnetic stirrer to maintain a uniform ion concentration, to disperse the Al_2O_3 nanoparticles and to reduce the localized heat accumulation.

A JEOL JSM-6460LV scanning electron microscope (SEM) was employed for observing the surface morphology of the coatings. The elemental composition of the surface layers was examined with an energy-dispersive spectrometer (EDS) that was part of the SEM. A BDX3300-type X-ray diffractometer (XRD) was also utilized to perform phase analyses of the anodizing films.

3 RESULTS

3.1 The variation of the voltage with the anodizing time

The curves of voltage versus time during the formation of the composite films in constant-current mode are shown in **Figure 2**. It is clear that the curve can be divided into three stages in the process of composite oxidation. During stage I, the voltage increases rapidly to 83 V during the first 20 s, with an increase rate of 3.32 V/s (**Figure 2**). The rapid voltage rise can be attributed to the formation of a dense insulating layer on the surface of the magnesium alloy after energizing. At this stage, there is no electrical discharge and only intensive oxygen evolution could be seen on the sample's surface. After 25 s, when the voltage reaches critical values, some weak parts of the oxide film are broken down and the micro-arc discharge occurs, corresponding to the initiation of the second stage of anodic oxidation. The critical voltage of the spark is called the breakdown voltage, which depends on the composition and the conductivity of the electrolyte.[21] Initially, small, dense

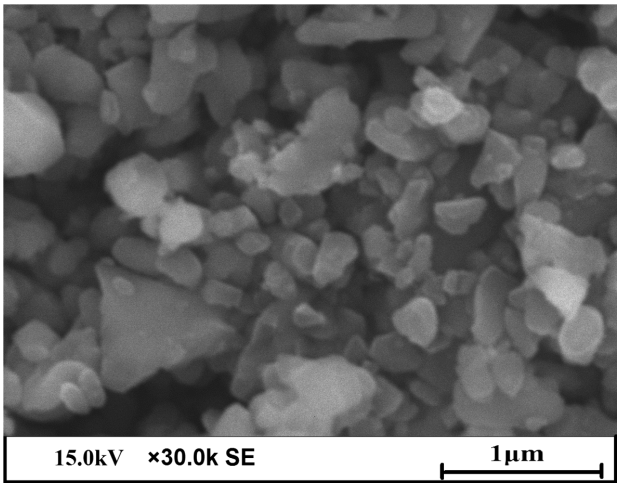

Figure 1: SEM image of used Al_2O_3 nanoparticles

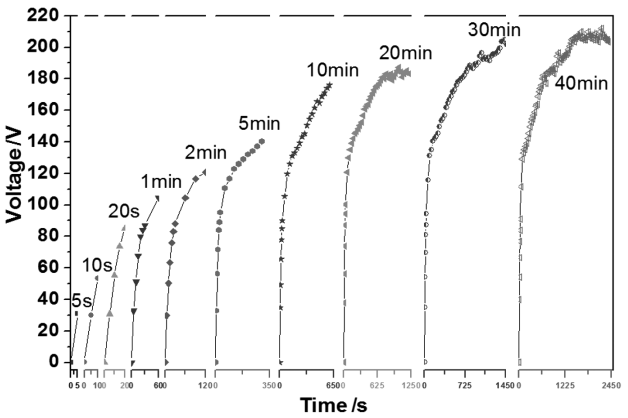

Figure 2: Voltage variation with time

and relatively short life sparks could appear on the edge of the specimens, and then spread to the entire surface. These sparks are accompanied by considerable gas evolution. At this stage, the voltage continues to increase as the oxidation time increases, but the growth rate drops to 0.15 V/s.

After 10 min, the voltage progressively moves into the third stage. At this stage, the voltage rises slowly and tends to be stable with large, sparse and long-life sparks found on the surface of the specimens. After 10 min, the termination voltage reaches about 200 V.

3.2 The variation of the voltage and the thickness of the anodic oxide films with time

Figure 3 is the change curve of the voltage and oxide film thickness with time during the anodization. It is clear that the thickness change of the anodic oxide films is consistent with the voltage variation with the anodizing time. When prolonging the oxidation time, the thickness of the oxide film could also be divided into three stages. (1) Compact and dense barrier layer growth stage (voltage less than 83 V): there is no spark on the surface of the alloy substrate during this stage and the film growth rate is up to 0.015 m/s. (2) Micro-spark oxide growth (83–189 V) stage: when the voltage is greater than the breakdown voltage of the anodic oxide film, the weak parts of the film produce small white sparks that move quickly on the specimen surface. The growth rate of the anodic oxide film in the area of the electric spark scanning is as high as 0.014 m/s, which is slightly smaller than the growth rate of the first stage. This is because the energy density applied on the oxide film increases constantly with increasing oxidation voltage, resulting in thickening of the oxide film. (3) Arc discharge oxide growth stage (>189 V): the big orange sparks appear on the surface of the AZ31 magnesium alloy and the duration of the spark is longer than the second stage. The spark density decreases drastically. From **Figure 3** it can be seen that the growth rate of the oxide film is slowing down. Based on a calculation, the oxidation film growth rate is 0.006 μm/s. This is related to the suppressed diffusion of ions by the thicker oxide films pre-formed on the specimen surface. When increasing the anodizing time, the solution temperature increases. The dissolution rate of the oxide film increases and the growth rate of the oxide film slows down.

3.3 Surface morphologies and compositions with time

Figure 4 shows the surface morphologies of the anodic composite films obtained on specimens at (5, 10, 20) s and (1, 2, 5, 10, 20, 30 and 40) min. The coating compositions at various points and areas selected on the specimen surface with different intervals are listed in **Table 1**. The composite oxide film generally consists of Mg, O, Si, Na and Al. The Mg comes from the matrix,

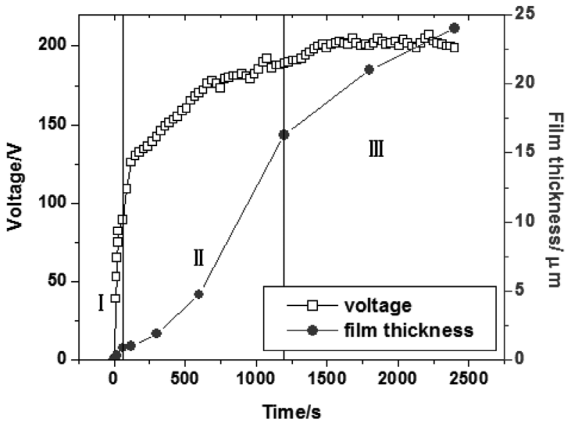

Figure 3: Thickness and voltage variation of the oxide films with anodizing time

and the elements O, Si, Na, and Al should be derived from the electrolyte.

From **Figures 4a** it can be seen that during the first 5 s only a few dispersed particles are observed on the specimen surface, with the other areas relatively flat and smooth. EDS analyses show that the content of Al in the particulate (point A) is as high as 6.71 *w*/%, which is much higher than that of the AZ31 magnesium alloy matrix. The Mg content is 70.4 *w*/%, with up to 20.96 *w*/% O, indicating that the particles are Al_2O_3 nanoparticles coated by magnesium oxide. A small amount of Na comes from the adsorption of the electrolyte. The content of Mg and O in the flat area (point B) is 95.03 *w*/% and 4.97 *w*/%, respectively, indicating that the flat area is dominated by the magnesium matrix.

At 10 s, in addition to some scattered particles, the specimen surface exhibits an island-like topography, and the particles have a tendency to expand and spread around. Other regions of the specimens are still relatively flat. The EDS results show that the Al content on the large particles (point C) increases to 21.92 *w*/% with enriching O as well, indicating that the Al_2O_3 nanoparticles are aggregated in the oxide films. The presence of 4.62 *w*/% Si confirms that the silicate electrolyte is also involved in the film's formation. The flat area (point D) is still dominated by magnesium, with a few O, suggesting the films are very thin.

After 20 s the islands formed on the specimen surface grow. Some small white particles are adsorbed on other flat areas of the specimen surface. The EDS results show that the island is mainly composed of MgO. A total of 2.01 *w*/% Al is detected at point E, which further proves that the anodic oxide film is formed by the Al_2O_3 nanoparticles adsorbed on the magnesium matrix. The flat regions (point F) contain 2.34 *w*/% Al, which indicates that the white particles in the flat area are Al_2O_3 nanoparticles absorbed on the magnesium matrix.

At 1 min the specimen surface is fully covered by anodic oxide films. The film morphology is inhomogeneous, with some flat and porous regions (**Figures 4d**), which might be attributed to the formation of an uneven

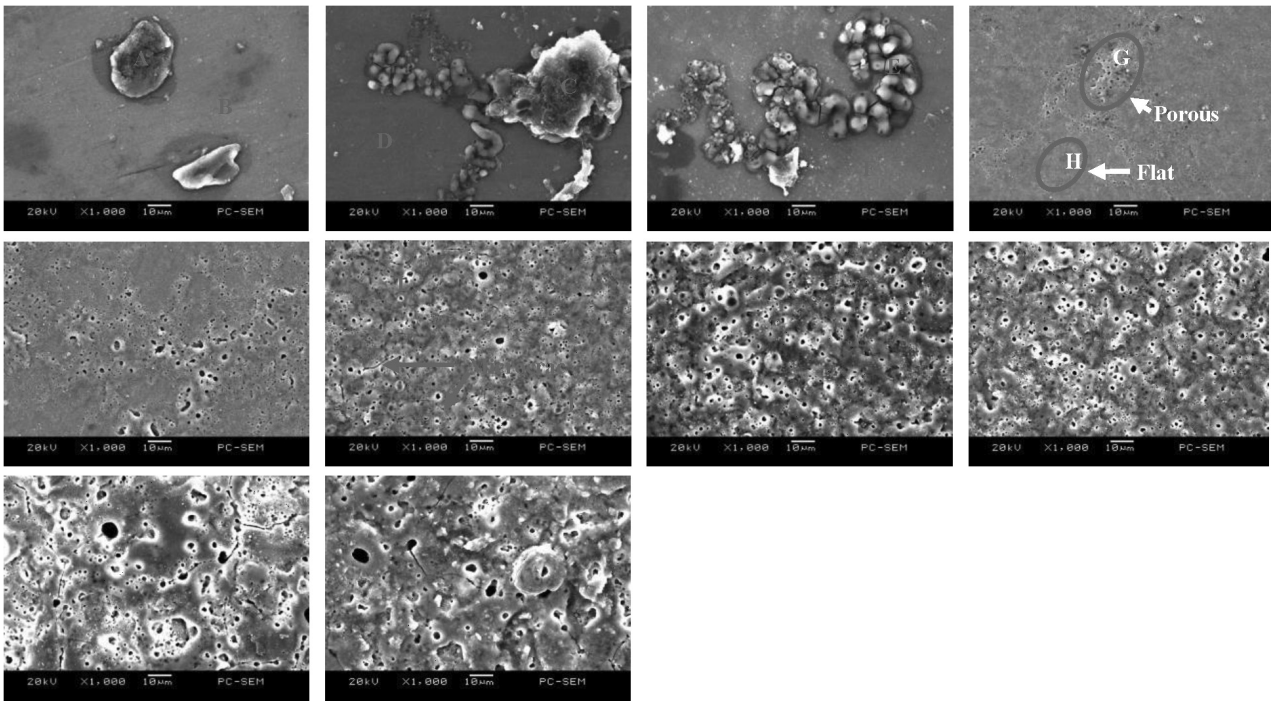

Figure 4: Micro-morphology of the oxide films after different anodizing times: a) 5 s, b) 10 s, c) 20 s, d) 1 min, e) 2 min, f) 5 min, g) 10 min, h) 20 min, i) 30 min, j) 40 min

coating.[22,23] The porous (point G) and flat regions (point H) are composed of O, Mg, Al and Si. There is a higher content of Al and a lower content of Si and O in the flat regions. This indicates that the adsorption capacity of the Al_2O_3 particles in this region is higher, while the oxidation is not enough. The contents of Si and O in the porous area are higher, with lower contents of Al and Mg, suggesting that the oxide film in the porous zone grows faster. The presence of Al and Mg indicates that the nanoparticles have always been involved in the growth of the oxide film.

After treating for 2 min, the areas of the porous region and their sizes increase. The specimen surface is fully covered by porous oxide films and a few micro-cracks after 5 min of anodizing. But the oxide film's uniformity is significantly enhanced, as shown in **Figure 4f**. The chemical compositions of the different points on the oxide film's surface are almost the same (as listed in **Table 1**). This small, uniform porous feature was maintained until oxidizing for 20 min. As the oxidation time prolongs, the micro-pore size continuously increases. For example, the largest micro-pore of the oxide films obtained after 30 min is 7 μm in diameter (**Figure 4i**), larger than that (about 2 μm) obtained after 20 min (**Figure 4h**). **Figures 4j** shows that after 40 min the oxide film's surface is rather rough. Particles and crater-like pores are formed on the anodic oxide film's surface.

Figure 5 shows high-magnification micrographs of the oxide films obtained after (5, 10, 20, 30 and 40) min. It is clear that after 5 min, many round holes with different sizes are present on the surface of the anodic oxide film, with a few nanoparticles uniformly dispersed. When increasing the oxidation time, the sizes of the surface micro-pores in the oxide films increase and the cracks gradually propagate, contributing to a larger surface roughness. The elemental compositions of the circled regions on the surface of the oxide coatings are detected by EDS and are listed in **Table 2**. It is clear that the concentration of Al in the particle-enriched region is higher than that in the matrix, and the particle size is also

Table 1: Compositions of the oxide films at different intervals

Anodizing time	Area	Element content (*w*/%)				
		O	Na	Mg	Al	Si
5 s	A	20.96	1.93	70.40	6.71	0.00
	B	4.97	0.00	95.03	0.00	0.00
10 s	C	48.16	5.55	19.75	21.92	4.62
	D	4.97	0.00	95.03	0.00	0.00
20 s	E	51.20	0.00	46.79	2.01	0.00
	F	8.08	1.24	88.34	2.34	0.00
1 min	G	29.82	0.00	63.16	0.90	6.12
	H	10.85	0.00	83.59	2.77	2.79
5 min	I	45.96	3.44	35.60	1.67	13.34
	J	46.91	3.70	33.92	1.82	13.65

Table 2: Compositions of the anodic coatings at different intervals

Anodizing time	Area	Element content (*w*/%)				
		O	Na	Mg	Al	Si
5 min	A	46.70	2.04	35.51	8.29	7.46
10 min	B	40.68	3.91	30.07	13.10	12.24
20 min	C	40.71	2.63	35.27	6.27	15.11
30 min	D	41.72	4.26	32.21	4.39	17.41
40 min	E	43.39	3.74	31.02	4.48	17.37

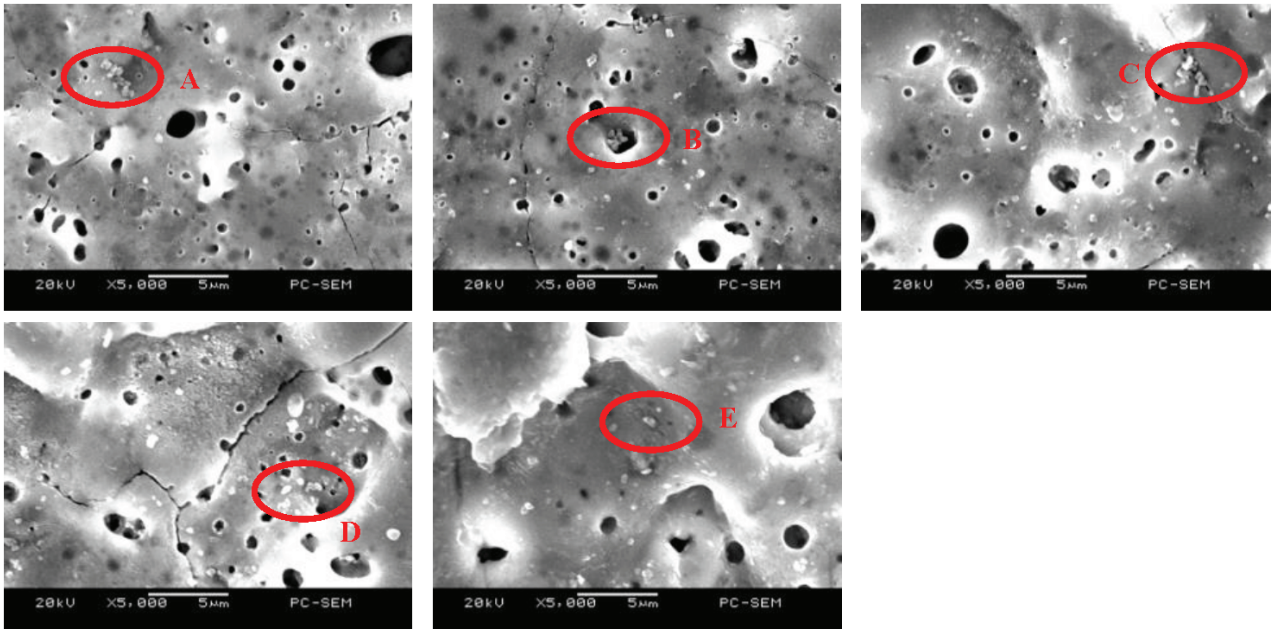

Figure 5: Micro-morphology of the oxide films at high magnification: a) 5 min, b) 10 min, c) 20 min, d) 30 min, e) 40 min

comparable with that of the nanoparticles added in the experiment, confirming that they correspond to the Al_2O_3 nanoparticles. With the prolongation of the treatment time, the content of O decreases and the content of Si increases, indicating that MgO was predominated in the early stage of oxidation. In the late stage of oxidation, more silicates participate in the reaction, leading to a slightly increased content of magnesium silicate on the oxide film surface. **Figure 5** shows that there are many white particles on the coating surface and some fill in the micro-pores, suggesting that the Al_2O_3 particles added to the electrolyte could not only be adsorbed onto the oxide film surface, but could also become entrapped into the film during anodizing.

According to the results of the surface morphology, the composite oxide film obtained after oxidation for 20 min is uniform and compact, and the micro-pores are fine and distributed uniformly. Therefore, to obtain a good protective effect on the surface of the AZ31 magnesium alloy, it is necessary to anodize for 20 min. A cross-sectional image of the composite anodic film after 20 min of oxidation is shown in **Figure 6**. It is clear that the film contains a number of micro-pores and particles in its interior, confirming the entrapment of the added Al_2O_3 particles in the film.

The XRD diffraction pattern of the composite oxide film after 20 min of oxidation is shown in **Figure 7**. It is clear that the composite coating is mainly composed of MgO, Mg_2SiO_4 and Al_2O_3 phases. A few Al_2O_3 peaks were detected in the oxide films, possibly due to its very low content.

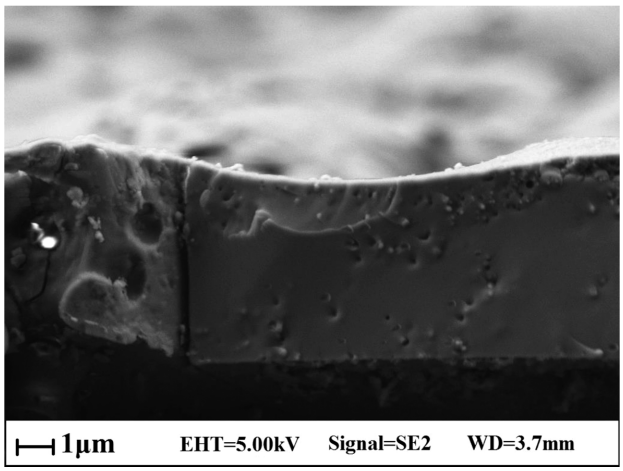

Figure 6: Cross-section profile of anodic oxide films with Al_2O_3 nanoparticles

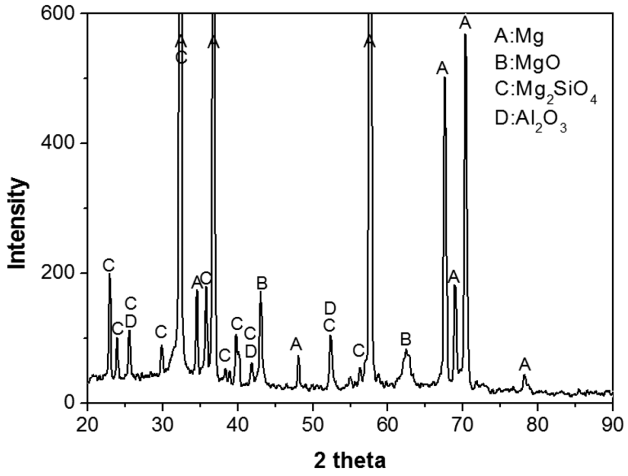

Figure 7: XRD patterns of the composite oxide coating anodized after 20 min

4 DISCUSSION

From the voltage-time curve in **Figure 2** it is clear that the addition of nanoparticles does not change the basic process of anodic oxidation of magnesium alloys, and the voltage-time curve is still composed of three stages.

According to the previous experimental results, we attempt to propose the following schematic (**Figures 8**) illustrating the growth behavior of the composite anodic oxidation film. The composite oxide film consists of a dense and compact barrier layer and a porous layer.[24] In the process of oxidation, the dense barrier layer is formed at the interface between the substrate and the electrolyte, then the porous layer grows on the dense barrier layer. Since the barrier layer is grown from the outside to the inside of the matrix,[25] it is not possible to include Al_2O_3 nanoparticles in the barrier layer of the oxide film. The oxide film is formed by O^{2-} (or OH^-) migrating to the interface between the substrate and the oxidation film , and by Mg^{2+} migrating to the interface between the oxidation film and the electrolyte.[26] The Al_2O_3 nanoparticles added into the electrolyte are modified with anionic surfactants. Hence, they have negative charges on the surface.[27] Under the action of the electric field force and magnetic stirrer mixing, the particles could move to the surface of the oxide film (the anode) during anodization. When the voltage between electrodes exceeds a certain critical value, some weak parts of the dense barrier oxide film are broken down, and the micro-area spark discharge occurs. There are numerous small white sparks on the surface of the substrate immersed in the electrolyte solution, and the porous film starts to be formed. Owing to the high temperature and high pressure caused by the spark discharge in the micro-area, the mutual diffusion of oxygen and magnesium ions in the film near the pore wall will be strongly promoted. Meanwhile, it will promote the drastic fluctuation of the molten magnesia so that part of the melt will be ejected outwards. The nano-Al_2O_3 particles on the surface of the substrate were wrapped by the molten materials that were ejected from the channels. After solidification of the molten materials, nano-Al_2O_3 and the molten materials became parts of the film. This fluctuation of the melt phase, combined with the physical effect of the magnetic stirring of the electrolyte, allows the Al_2O_3 particles to enter the interior of the oxide film. According to Matykina et al.,[28] the presence of the nanoparticles on the surface is due to the transport from the inner coating through the discharge channels or to an electrophoretic effect owing to the electric field in the electrolyte. The particles suspended in the electrolyte could be incorporated into the micropores of the oxide layer, as also observed by other authors.[29,30] Meanwhile, since the porous film has excellent adsorbability, the Al_2O_3 particles could be adsorbed by the porous surface of the film through mechanical capture, adsorption, and chemical co-actions.

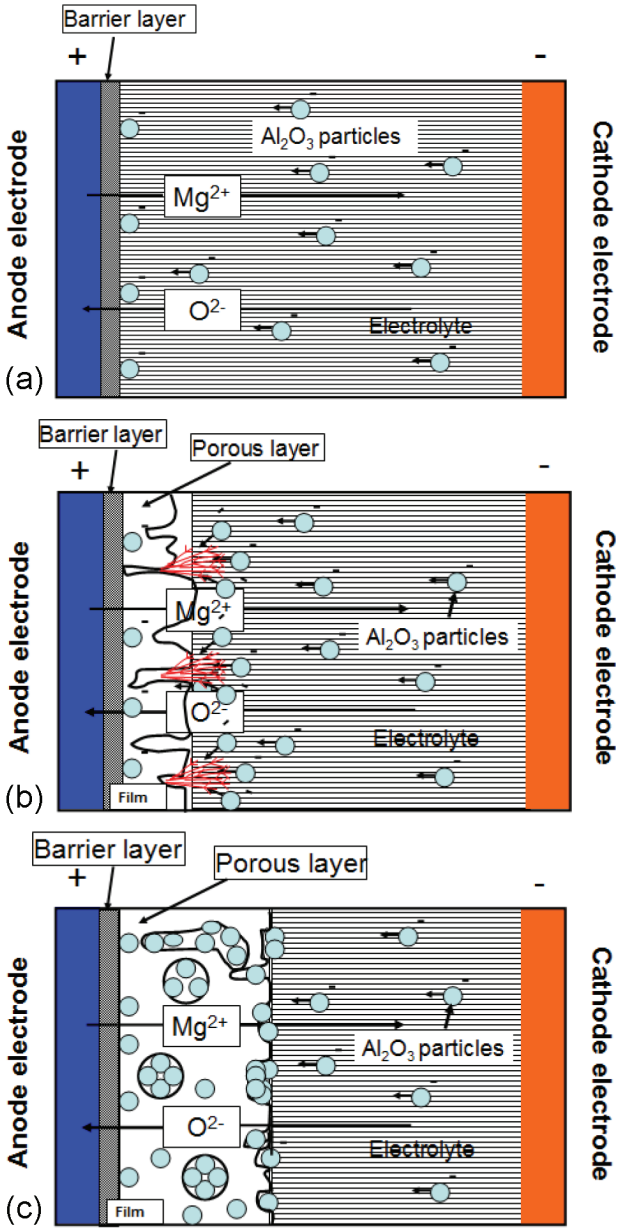

Figure 8: Schematic illustrating the formation of the composite oxidation film during the anodization

Combined with the surface morphology at high magnification and the cross-sectional morphology of **Figure 5** and **Figure 6**, we propose that the state of the particles kept in the films might be as follows: (1) some Al_2O_3 particles are adsorbed on the oxide film surface (as shown in **Figures 5a**, **5d**, **5e**); (2) other Al_2O_3 particles are incorporated into larger holes and cracks in the oxide film (**Figures 5b**, **5c**); (3) there are some particles by the discharge channel of the molten magnesium oxide wrapped in the oxide film (**Figure 6**). The presence of these nanoparticles in the oxide film changes the composition, morphology and structure of the oxide film, leading to a greatly improved performance of the oxide film.

5 CONCLUSIONS

(1) The addition of Al_2O_3 nanoparticles does not change the basic process of the anodic oxidation of magnesium alloys. The thickness change of the oxide films is consistent with the voltage variation with oxidation time.

(2) At the initial stage of oxidation, the oxide film coated with nanoparticles on the substrate surface grows to show an island-like morphology. After anodizing for 5 min, the porous film completely covers the substrate and the oxide film begins to grow uniformly. With prolonging of the oxidation time, the oxide film is thickened with increased pore sizes. In addition, the film changes from compact to porous and finally to a greatly roughened morphology with many particles.

(3) The phase composition of the composite coating is periclase MgO, forsterite Mg_2SiO_4 and α-Al_2O_3.

(4) Al_2O_3 nanoparticles mainly exist in three forms in the composite oxide film: a) some Al_2O_3 particles are adsorbed on the oxide film surface; b) other Al_2O_3 particles are adsorbed in the micro-pores in the porous layer of the oxide film; c) there are also some particles trapped in the oxide film through the discharged channel. These nanoparticles in the oxide film change the chemical composition, morphology and the structure of the oxide film, contributing to a greatly improved performance of the oxide film.

Acknowledgements

The present work was supported by the Fundamental and Cutting-edge Research Plan of Chongqing (Grant no. cstc2016jcyjA0434) and Scientific and Technological Research Program of Chongqing Municipal Education Commission (KJ1601104, KJ1600924).

6 REFERENCES

[1] V. Ezhilselvi, J. Nithin, J. N. Balaraju, S. Subramanian, The influence of current density on the morphology and corrosion properties of MAO coatings on AZ31B magnesium alloy, Surface and Coatings Technology, 288 (**2016**), 221–229, doi:10.1016/j.surfcoat.2016.01.040

[2] J. Joost. William, P. E. Krajewski, Towards magnesium alloys for high-volume automotive applications, Scripta Materialia, 128 (**2017**), 107–112, doi:10.1016/j.scriptamat.2016.07.035

[3] J. L. Liu, H. J. Yu, C. Z. Chen, F. Weng, J. J. Dai, Research and development status of laser cladding on magnesium alloys: A review, Optics and Lasers in Engineering, 93 (**2017**), 195–210, doi:10.1016/j.optlaseng.2017.02.007

[4] S. Nezamdoust, Z. D. Seifzadeh, Z. Rajabalizadeh, PTMS/OH-MWCNT sol-gel nanocomposite for corrosion protection of magnesium alloy, Surface and Coatings Technology, 335 (**2018**), 228–240, doi:10.1016/j.surfcoat.2017.12.044

[5] N. V. Phuong, M. Gupta, S. M. Moon, Enhanced corrosion performance of magnesium phosphate conversion coating on AZ31 magnesium alloy, Transactions of Nonferrous Metals Society of China, 27 (**2017**), 1087–1095, doi:10.1016/S1003-6326(17)60127-4

[6] H. Jeong, J. D. Cho, Characterization of interfacial layers grown between magnesium substrates and SiOx films deposited by plasma-enhanced CVD, Surface and Coatings Technology, 332 (**2017**), 105–111, doi:10.1016/j.surfcoat.2017.07.088

[7] J. E. Gray, B. Luan, Protective coatings on magnesium and its alloys - a critical review. Journal of Alloys and Compounds, 336 (**2002**), 88–113, doi:10.1016/S0925-8388(01)01899-0

[8] W. Yang, D. P. Xu, X. F. Yao, J. L. Wang, J. Chen, Stable preparation and characterization of yellow micro arc oxidation coating on magnesium alloy, Journal of Alloys and Compounds, 74 (**2018**), 609–616, doi:10.1016/j.jallcom.2018.02.192

[9] S. Y. Jian, J. L. Lee, H. B. Lee, H. H. Sheu, C. Y. Ou, D. G. Ming, Influence of electroless plating on the deterioration of the corrosion resistance of MAO coated AZ31B magnesium alloy, Journal of the Taiwan Institute of Chemical Engineers,68 (**2016**), 496–505, doi:10.1016/j.jtice.2016.09.040

[10] S. M. Li, M. Q. Zhu, J. H. Liu, M. Yu, L. Wu, J. D. Zhang, H. X. Liang, Enhanced tribological behavior of anodic films containing SiC and PTFE nanoparticles on Ti_6Al_4V alloy, Applied Surface Science, 316 (**2014**), 28–35, doi:10.1016/j.apsusc.2014.07.088

[11] X. P. Lu, S. Mauricio, B. Carsten. Formation of photocatalytic plasma electrolytic oxidation coatings on magnesium alloy by incorporation of TiO_2 particles, Surface & Coatings Technology, 307 (**2016**) A, 287–291, doi:10.1016/j.surfcoat.2016.09.006

[12] H. Li, Y. Z. Sun, J. Zhang, Effect of ZrO_2 particle on the performance of micro-arc oxidation coatings on Ti_6Al_4V, Applied Surface Science, 342 (**2015**), 183–190, doi:10.1016/j.apsusc.2015.03.051

[13] M. Mohedano, C. Blawert, M. L. Zheludkevich, Silicate-based Plasma Electrolytic Oxidation (PEO) coatings with incorporated CeO_2 particles on AM50 magnesium alloy, Materials & Design, 86 (**2015**), 735–744, doi:10.1016/j.matdes.2015.07.132

[14] Y. Wang, D. B. Wei, J. Yu, S. Di, Effects of Al_2O_3 nano-additive on performance of micro-arc oxidation coatings formed on AZ91D Mg alloy, Journal of Materials Science & Technology, 30 (**2014**) 10, 984–990, doi:10.1016/j.jmst.2014.03.006

[15] Q. Z. Chen, Z. Q. Jiang, S. G, Tang, W. B. Dong, Q. Tong, W. Z. Li, Influence of graphene particles on the micro-arc oxidation behaviors of 6063 aluminum alloy and the coating properties, Applied Surface Science, 423 (**2017**), 939–950, doi:10.1016/j.apsusc.2017.06.202

[16] A. C. Ciubotariu, L. Benea, L.V. Magda, V. Dragan, Electrochemical impedance spectroscopy and corrosion behaviour of Al_2O_3–Ni nano composite coatings, Electrochim Acta, 53 (**2008**) 13, 4557–4563, doi:10.1016/j.electacta.2008.01.020

[17] D. F. Zhang, Y. N. Gou, Y. P. Liu, X. X. Guo, A composite anodizing coating containing superfine Al_2O_3 particles on AZ31 magnesium alloy, Surface & Coatings Technology, 236 (**2013**) 2, 52–57, doi:10.1016/j.surfcoat.2013.04.059

[18] D. F. Zhang, Y. N. Gou, H. Yang, X. X. Guo, The effect of nano-Al_2O_3 particles to anodic oxidation on magnesium alloy, Journal of Functional Materials, 44 (**2013**) 14, 2018–2022, doi:10.3969/j.issn.1001-9731.2013.14.010

[19] Y. N. Gou, D. F. Zhang, D. Yi, C. Y. Zhang, The effect and mechanism of amion acid on the anodic oxidation of magnesium alloy, Rare Metal Materials and Engineering, 46 (**2017**) 4, 1103–1109

[20] Y. N. Gou, Y. Y, Su, C. Jiang, W. Q. Hua, E. Zhang, X. Yu, Effect of electrolytes components on properties of composite anodizing oxidation coatings on magnesium alloy, Hot Working Technology, 46 (**2017**) 10,151–154

[21] S. Ikonopisov, Theory of electrical breakdown during formation of barrier anodic films, Electrochimica Acta, 22 (**1977**) 10, 1077–1082, doi:10.1016/0013-4686(77)80042-X

[22] R. F. Zhang, S. F. Zhang, Formation of micro-arc oxidation coatings on AZ91HP magnesium alloys, Corrosion Science, 51 (**2009**) 12, 2820–2825, doi:10.1016/j.corsci.2009.08.009

[23] W. P. Li, M. Q. Tang, L. Q. Zhu, H. C. Liu, Formation of microarc oxidation coatings on magnesium alloy with photocatalytic performance, Applied Surface Science, 258 (**2012**) 24, 10017–10021, doi:10.1016/j.apsusc.2012.06.066

[24] X. M. Chen, C. P. Luo, J. W. Liu, Structure analysis of micro-arc oxidation on magnesium alloy, China Surface Engineering, 22 (**2009**) 5, 45–49

[25] Z. Y. Zhang, Q. Zhao, N. Chen, Growth of ceramic coating via micro-arc oxidation on magnesium alloy, Electroplating & Finishing, 26 (**2007**) 7, 5–8

[26] S. Y. Chen, C. Kang, J. Wang, C. S. Liu, K. Sun, Synthesis of anodizing composite films containing superfine Al_2O_3 and PTFE particles on Al alloy, Applied Surface Science, 256 (**2010**) 22, 6518–6525, doi:10.1016/j.apsusc.2010.04.040

[27] S. Y. Wang, N. C. Si, Y. P. Xia, L. Liu, Influence of nano-SiC on microstructure and property of MAO coating formed on AZ91D magnesium alloy, Trans. Nonferrous Met. Soc. China, 25 (**2015**) 6, 1926–1934, doi:10.1016/S1003-6326(15)63800-6

[28] E. Matykina, R. Arrabal, F. Monfort, P. Skeldon, G. E. Thompson, Incorporation of zirconia into coatings formed by DC plasma electrolytic oxidation of aluminium in nanoparticle suspensions, Applied Surface Science, 255 (**2008**) 5, 2830–2839, doi:10.1016/j.apsusc.2008.08.036

[29] Y. Q. Wang, X. J. Wang, W. X. Gong, K. Wu, F. H. Wang, Effect of SiC particles on microarc oxidation process of magnesium matrix composites, Applied Surface Science, 283 (**2013**), 906–913, doi:10.1016/j.apsusc.2013.07.041

[30] Q. Z. Chen, Z. Q. Jiang, S. G. Tang, W. B. Dong, Q. Tong, W. Z. Li, Influence of graphene particles on the micro-arc oxidation behaviors of 6063 aluminum alloy and the coating properties, Applied Surface Science, 423 (**2017**), 939–950, doi:10.1016/j.apsusc.2017.06.202